INTERNATIONAL JOURNAL OF HYDROGEN ENERGY 42 (2017) 30569–30583

Available online at www.sciencedirect.com

ScienceDirect

journal homepage: www.elsevier.com/locate/he

Experimental analysis of photovoltaic integration with a proton exchange membrane electrolysis system for power-to-gas

John Stansberry, Alejandra Hormaza Mejia, Li Zhao, Jack Brouwer *

Advanced Power and Energy Program, University of California, Irvine, CA 92697-3550, USA

ARTICLE INFO

Article history:
Received 31 August 2017
Received in revised form
13 October 2017
Accepted 30 October 2017
Available online 22 November 2017

Keywords:
Proton exchange membrane electrolyzer
Electrolysis
Solar photovoltaic
Power-to-gas
Renewable hydrogen

ABSTRACT

A proton exchange membrane electrolyzer is integrated with a photovoltaic system using Maximum Power Point Tracking (MPPT) power electronics systems in several configurations to evaluate the extent to which the system can respond to the dynamics of photovoltaic power. Both direct current from the solar photovoltaics (DC) and alternating current rectified to DC from the grid (AC) configurations are evaluated and the overall efficiency and dynamic hydrogen production capabilities are assessed. Performance characteristics as a function of weather (winter vs. summer; cloudy vs. sunny) and as a function of operating conditions (e.g., ambient temperature, stack temperature) are evaluated. The direct DC configuration was found to provide the highest energy transfer efficiency from electrical power to hydrogen, with a relative increase of 7–8% compared to the AC configuration. The grid-connected AC configuration produced a baseline case to compare the characteristic losses, efficiency, and dynamics of the PV integrated DC case. The highly dynamic PV production during cloudy weather was handled by the system, accommodating input power ramp rates as high as 1270 W/s, and part load conditions as low as 7.6% of rated power. Transient operation exhibited small performance degradation compared to steady solar conditions. Hydrogen production was more efficient for high stack operating temperatures and high ambient temperatures.

Introduction

Background

Rising greenhouse gas emissions coinciding with increasing global energy demands have brought the need for more carbon neutral power generation sources. Renewable sources of energy such as wind and solar have the greatest potential in meeting this need. Additionally, they are attractive in that they offer a renewable solution in the face of dwindling energy resources such as fossil fuels. In 2014, solar and wind power generators were the two fastest growing sources of renewable electricity in the United States; wind energy comprised 27% of total electricity generation capacity additions, and large solar energy installations (greater than 1 MW capacity) comprised 22% [1].

Solar and wind power generators face challenges with their intermittency and uncontrollability that can lead to curtailment as market penetration rises [2]. Curtailment refers to the

* *Corresponding author.*
E-mail address: jbrouwer@uci.edu (J. Brouwer).
https://doi.org/10.1016/j.ijhydene.2017.10.170

intentional reduction in output of a solar or wind generator because it is not needed at that moment due to overgeneration, effectively "wasting" the power generation [3]. Overgeneration occurs whenever the solar or wind output becomes greater than the grid demands in any specific location or moment in time. California's electrical grid is already experiencing the challenges of high market penetration of solar and wind power that is leading to renewable energy curtailment. In one particular event on March 23, 2015, renewable energy generators had 1142 Megawatts of power curtailed for over 90 min, comprising enough power for hundreds of thousands of residences during this period [4]. With California's SB350 pushing for even greater renewable power use (50% renewable energy sources are required by this new law), more than double the current amount of renewable resources will be installed there [5]. Solar and wind capacity have been identified as needing to comprise a large share of this high renewable energy portfolio [6]. As a result, overgeneration of variable renewable energy resources will be an inevitable consequence of any highly renewable electricity system [3]. This was the case discovered in a study considering a renewable portfolio standard (RPS) of 50% in California [7], a high RPS case for the United States eastern interconnection regional transmission organization PJM [8], and a study of 100% RPS cases in the Australian National Electricity Market [9]. With these policies in California and around the world, large amounts of energy storage will become an absolute necessity in the future, more renewable utility grid network.

Tarroja et al. determined that high renewable penetration levels would impose 'severe challenges' for load balancing costs and operation in lieu of any 'energy management strategies' [10]. A promising strategy to mitigate the intermittency of wind and solar is energy storage [11]. Energy storage brings to the electrical grid the capability to decouple the temporal aspects of electrical generation versus demand. Conventional energy storage technologies include battery, fly wheel, compressed air, and pumped hydro.

For the purposes of energy storage technologies in capturing renewable energy resources, there are several critical attributes desired. For instance, these storage technologies should be efficient, must be able to meet high charge/discharge rates, and must exhibit fast ramping capabilities. Especially when very high renewable power use is required, the storage solutions must also be able to store tremendous amounts of energy. Combined with the challenging power demand dynamics of any massive electrical grid, appropriate grid scale energy storage technology needs to have as high response times as possible, together with the appropriate energy and power storage capacities to handle instantaneous, hourly, diurnal, and seasonal storage requirements [12].

One archetype of energy carrier that meets some of the energy storage criteria is chemical energy storage. Fig. 1 describes the available sustainable energy storage technologies that various electric utility scale organizations are considering to support grid integration of renewables. Synthetic natural gas (SNG) and Hydrogen (H_2) are the clear frontrunners in the massive energy storage and long discharge time range of storage technologies. This is because these technologies offer independent sizing of the system energy and power capacity. The use of these technologies enables storage of large amounts of energy in existing storage, transport, and conversion resources (e.g., use existing caverns and pipelines for gas storage, the natural gas system for energy transport, and existing high-efficiency fuel cells or combined cycle gas power plants to return electricity).

Power-to-gas is a concept wherein a chemical energy carrier is produced during peak renewable power production periods. This potentially provides frequency regulation and voltage support ancillary services, in addition to reducing the

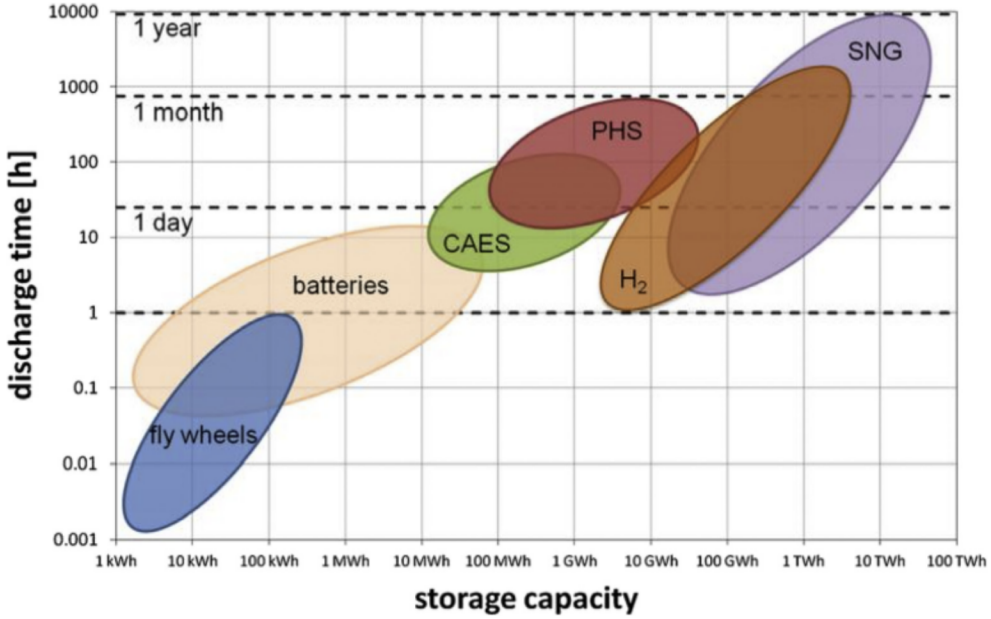

Fig. 1 – Comparison of energy storage technologies [13].

stress on balancing thermal power plants and any associated carbon emissions penalties during low renewable generation hours. Excess generation events that end in curtailment of solar and wind plants impede low-carbon generation goals. Power-to-gas provides a new energy pathway that reduces the need for curtailment. In comparison to other energy storage technologies, power-to-gas has been found to be desirable at grid scale applications when energy storage, energy portability, and the ability for seasonal storage are sought after [13]. Power-to-gas is a relatively new technology concept that has come about with the increased apparent need for long term energy flexibility. A 2012 review of power-to-gas pilot plants found 26 demonstration plants in operation worldwide, 95% of which were found in either Europe or North America [14].

The primary electrochemical conversion process in many power-to-gas concepts is water electrolysis. In water electrolysis, an electric potential across two electrodes drives a water splitting process that generates hydrogen and oxygen. The electrodes and products are separated by an electrolytic layer that conducts ions across from one electrode to the other. Hydrogen is produced in the cathode compartment and oxygen is produced in the anode compartment. There are a number of different electrolyzer technologies available today, distinguished by the type of electrolyte employed.

Unlike traditional batteries, another form of electrochemical conversion device, electrolyzers produce energy that is not stored within the conversion device itself. Instead the energy is stored outside of the conversion device in a separate storage device (e.g., tank, salt cavern) as hydrogen. Batteries store energy into the electrolyte and produce power from the same electrolyte stored between the two electrodes. Electrolyzers can continuously operate under load at a power level that can be independently designed from the amount of energy that the system can store, as long as the produced gases are able to be removed – stored or used. Batteries are limited by the fact that the same electrodes must either absorb or produce power at a capacity that is linked to the mass of active electrode material contained within the battery.

Hydrogen energy storage has the capability to deliver large energy capacities and/or power in and out over long periods of time, making it an attractive solution for grid scale energy storage. Maton et al.'s simulations on salt cavern based compressed hydrogen energy storage suggested that load shifting on daily time scales up to as long as seasonal time scales could be accomplished [15]. For solar energy the capability of load shifting on seasonal time scales to offset the dramatic difference in generation from summer to winter is particularly attractive [16]. Hydrogen produced renewably can be sent to several different pathways (see Fig. 2). Hydrogen can be injected directly into pre-existing natural gas infrastructure up to acceptable concentration levels, or used in methanation processes to generate carbon neutral methane for injection into natural gas infrastructure indefinitely. Alternatively, hydrogen can be stored separately for end use in fueling stations for transportation vehicles or for power generation in a fuel cell or combustion engine (Fig. 2).

Purpose

To realize the benefits of power-to-gas, the electrolysis system needs to be able to meet a number of criteria. Due to the intermittent nature of the renewable energy inputs, a wide range of part load condition operation and rapid dynamic response in a load following manner are desired. High efficiencies are needed to effectively capture renewable energy and keep operating costs down. Economic viability is a concern, with electrolyzer capital costs that are relatively high compared to similar sized energy storage options with more maturity [17].

Proton exchange membrane (PEM) electrolyzers are a relatively young electrolysis technology, with the first occurrence of the technology coming out of General Electric in the late 1960s [18]. The electrolyte membrane for which it is named consists of a solid polymer of the perfluorosulfonic acid family, with carbon-supported platinum electrocatalyst layers on each side, which allows for dissociation of cations when wet and the subsequent transport of hydrogen ions (H^+) across the membrane [19]. PEM electrolyzers are low temperature systems that are typically operated below 100 °C as the membrane must be hydrated to facilitate ion conduction. In lab environments, PEM stack efficiencies have been demonstrated as high as 85% higher heating value [20,21]. State of the art commercial PEM electrolyzer system efficiencies at large scale are found typically between 67% and 75% higher heating value [22].

Publications on PEM technology are more often concerned with Proton Exchange Membrane fuel cell systems, but within the last decade an increase in interest towards PEM

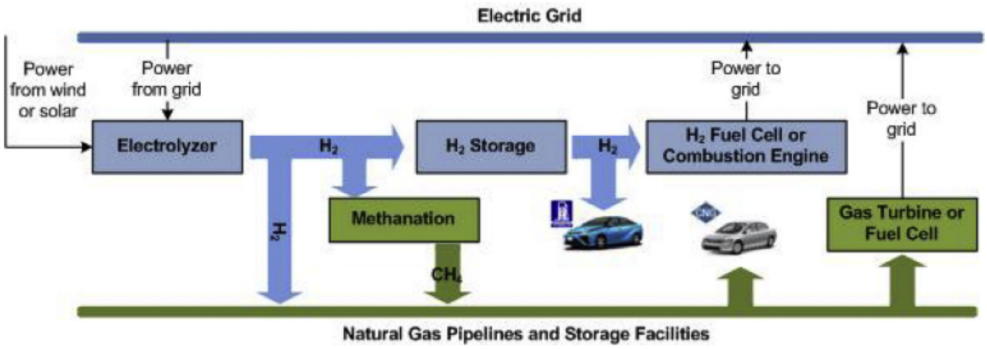

Fig. 2 – Power-to-gas concept – energy pathways for hydrogen energy storage integration.

electrolyzer can be observed in the greater proportion of publications concerning PEM electrolyzer systems [23]. A number of modeling approaches have been able to analytically characterize the theoretical effects of varying operating conditions and physical design characteristics on cell and stack performance and shown good agreement with experimental data [24–31]. Other efforts have also successfully characterized system level performance, incorporating the balance-of-plant to their models and having similar success with matching experimental system data [32,33]. Further analytical studies have demonstrated the suitability of PEM electrolyzer systems integrated with variable renewable energy for the production of renewable hydrogen [34–37] and further applied to a self-sustaining renewable hydrogen fueling station [38], reversible or 'regenerative' PEM fuel cell systems [39–41], and large scale power-to-gas scenarios [42]. Experimental studies have demonstrated the application of these systems for integration with variable renewable energy resources [43], in providing ancillary grid services [44], and have investigated the ability to electrochemically compress hydrogen in the electrolyzer stack, reducing or negating the requirement of additional compression equipment [45].

Proton Exchange Membrane electrolyzers show promising qualities for implementation with the power-to-gas concept [46]. These systems can operate at part load capacities as low as 5% up to 100% without interruption [47]. They have shown the capability to load follow highly dynamic power inputs, as would be necessary for integration with solar or wind energy sources [47]. These are important qualities for successful power-to-gas integration with solar due to the likely need for relatively low capacity factors of the electrolyzer systems when utilized for absorbing large amounts of solar over-generation [16]. Furthermore, solar photovoltaics output direct current (DC) electricity which enables the potentially attractive route of using that DC electricity directly towards electrolysis in a PEM electrolyzer, a DC electricity process. Conventional photovoltaic systems are coupled with inverters that take the DC electricity output and convert the electricity to grid acceptable alternating current (AC) electricity for ease of use. When coupling photovoltaic systems with electrolysis, the inclusion of an inverter adds unnecessary electrical conditioning steps and potentially greater losses as the electrical power is converted between DC to AC and back to DC when it reaches the electrolysis process. Direct coupling of solar photovoltaic panel systems with a PEM electrolyzer has been demonstrated by way of both 'hard wiring' photovoltaic system voltage to match the voltage of the electrolysis process [48] and using DC/DC power electronics to achieve the interconnection [43].

This study experimentally assesses performance metrics of a Proton Exchange Membrane electrolysis system that are critical to power-to-gas implementation. This system is uniquely configured with the ability to power the electrolysis process directly from a DC power source via the use of a DC/DC 'buck converter', using maximum power point tracking (MPPT) algorithm based power electronics to optimize photovoltaic to electrolysis process performance. System and stack efficiencies, dynamic capabilities, as well as common failure states were major targets for investigation. The efficacy of DC electricity usage 'directly' from a solar photovoltaic array to the electrolysis process is explored as well. In this case, characteristic system losses are compared to an AC to DC conditioning step that would be necessary with many commercial photovoltaic systems that output AC electricity for grid interconnection.

Experimental materials

The primary components of this study are a Uni-Solar 5000 W amorphous silicon photovoltaic array tied into a Proton OnSite HOGEN RE40 Proton Exchange Membrane Electrolyzer, hydrogen storage tanks, and data acquisition equipment.

HOGEN RE40

The Proton OnSite HOGEN RE40 is a differential pressure proton exchange membrane electrolyzer system rated for 7000 W of AC power consumption. The system was provided via loan agreement with Xcel Energy in support of the Southern California Gas Company's Power-to-Gas Demonstration at the National Fuel Cell Research Center. This particular system had served previously at the National Renewable Energy Laboratory for their Wind2H2 program [49]. A similar system was utilized in a photovoltaic to electrolysis optimization study by General Motors in Michigan, United States [48], and in a previous study at the National Fuel Cell Research Center [50].

The "RE" version of the system is a modification of a previous Proton Onsite commercial system, intended as a renewable energy research platform. In addition to the ability to operate off of single phase grid power 200–240 V AC (VAC) at 50/60 Hz up to 10000 W, the HOGEN RE is rated for a DC input between 60 and 200 V DC (VDC), up to 150 amps DC (ADC) for a maximum power of 10000 W.

The system has two modes of operation, a 'grid-only' mode, and a 'PV-only' mode. In the grid-only mode, a rectifier circuit takes the single-phase grid power input and rectifies and conditions it to DC for the electrolysis process. In PV-only mode, the electrolysis process is fed by a DC power source through a DC-DC 'buck converter' that steps down the voltage for the electrolysis process, which operates in a range of 26–60 VDC.

At full throughput, the system can deliver 1.16 normal cubic meters per hour (NM^3/hr) of hydrogen gas at a purity of 99.9995%> up to 1500 kPa. To achieve this level of purity, a two column pressure swing adsorption gas dryer process takes in wet hydrogen one column at a time. While one column is drying, the other column depressurizes and then 'vents' water and other impurities using a portion of the hydrogen stream, resulting in a ~10% parasitic loss of total hydrogen output. This venting action results in intermittent hydrogen flow as the solenoid valves controlling the dryer bed flow switch and a portion of the pressurized hydrogen stream is used to 'purge' a dryer bed. This purge event occurs about every 7–8 min under mid-range to full load.

The electrolyzer requires deionized (DI) water at a minimum purity of ASTM type II standards, for a resistivity of >1.0 MΩ-cm at an average consumption rate of 0.5 L/day. Proton Onsite recommends ASTM Type I water at a resistivity

of 18.2 MΩ-cm for minimal stack degradation. A milli-Q water purification system at the University of California Irvine's Metrohm Lab was used to supply 18.2 MΩ-cm via a 19 L polypropylene tank. DI water was fed from reservoir to tank by way of peristaltic pump and polypropylene hose to maintain water purity. DI water is stored in the system in two locations, the H_2O/H_2 separator 'A200' tank and the H_2O/O_2 separator 'A300' tank. Both tanks must be at a 'high' state of fill, checked by level switch, for the system to start. The electrolyzer can hold up to 7.6 L of water at any given time.

The cell stack is comprised of 20 cells each with an active area of 92.9 cm^2, a voltage range of 1.3–3 VDC, and a maximum current density of 74.8 mA/cm^2. This amounts to an active area of 1858 cm^2, with an operating range of 26–60 VDC across the stack up to 139 ADC. At maximum production, the system consumes up to 7000 W in PV-only mode, and up to 8000 W in Grid-only mode. The stack will operate in a temperature range from 5 °C up to 60 °C, measured via thermocouple on the water outlet of the stack.

Regardless of operational mode, ancillary loads are always powered via the grid to ensure stability. Typical ancillary power demand during electrolysis is around 450–500 W AC (WAC). A good portion of this power demand, ~300 WAC, goes to a blower which provides convective cooling to a radiator on the water feed and cabinet purge to keep the cabinet free of gas accumulation. Other necessary ancillary services include a water circulation pump, a hydrogen gas sensor, solenoid valves, pressure transducers, level switches, thermocouples, flow sensors, conductivity sensors, a backpressure regulator, relays, disconnects, an AC/DC rectifier (if in Grid-only) and the control board.

In PV-only mode, a maximum power point tracking (MPPT) controller integrated with a DC-DC 'buck converter' draws power from the DC power source, in this case the intended source of a photovoltaic (PV) array, to ensure the PV array is operating at its most efficient current and voltage point at all times. DC input voltage is stepped down from a nominal range of 60–200 VDC to the stack voltage set point to drive the electrolysis process. No PV power is used by other system processes.

Photovoltaic array

The Uni-Solar amorphous silicon photovoltaic array employed in this study is located on a 15° tilt roof facing in a south by southeast direction on the top of the Engineering Laboratory Facility at the University of California, Irvine. It covers an area 12.98 m by 8.47 m for a total coverage of 110 m^2. The array went into service on May 14, 1998 and has historically been tied into the building via a Trace SW5548 inverter, outputting at single phase 120 VAC directly to the local grid. Typically the array is wired in a manner that is rated at a voltage of 49.5 VDC at 124.8 ADC to optimize inverter performance. Using PVUSA test conditions (PTC), the nominal output of the system is roughly 4900 W DC into the inverter. The circuit for the PV array consists of 32 strings in parallel each comprised of one ASR-64 Watt panel in series with an ASR-128 Watt panel.

For the purposes of this study, the PV array was reconfigured to two ASR-64 Watt panels in series with two ASR-128 Watt panels for a total of 16 parallel strings. Effectively this doubles the maximum power operating voltage to 99 V and halves the current to 62.4 amps so that the PV array output is within the acceptable voltage range for the DC-DC converter system input on the HOGEN RE40.

Data acquisition

Fig. 3 summarizes the layout of the electrolyzer test bed. The HOGEN RE40 has an internal data stream that contains system pressure (kPa) and product pressure (kPa), which are the outputs from pressure transducers located on both sides of a backpressure regulator on the outlet of the hydrogen dryer. The former is the pressure inside the system up to the process connection, and the latter is the process pressure of the hydrogen delivered. Additionally, the system provides hydrogen flow rate (NM^3/hr), the system temperature (°C) measured from the water feed out of the cell stack, the cell stack voltage (volts), the cell stack current (amps), the DI water resistivity for quality monitoring (MΩ-cm), and the hydrogen gas concentration in the cabinet (%) to ensure that it never nears combustible levels.

A Brooks Mass Flow Controller (Model 8581i) was added on the process out stream to measure actual hydrogen flow rate, as the flow rate given by the HOGEN RE40 was a calculated value based upon measured current density, and not a flow rate measurement. Since the hydrogen dryers lose a not insignificant amount of hydrogen in their operation cycle, the additional metering quantifies the actual 'usable' quantities of hydrogen produced by the system. The mass flow controller was calibrated using a Meriam laminar flow element (Model 50MJI-6410). The analog signal from the mass flow controller was sent to a Seeed Studio Seeeduino microcontroller and converted to a digital signal which was logged by a serial monitor on the PC connected to the HOGEN RE40.

The single phase 200–240 VAC grid input to the HOGEN RE40 system was monitored using a Dent Elitepro recording polyphase power meter in conjunction with a current transformer. The power meter is able to record voltage, current, power (W), and power factor and log the data to a.csv file format that was exported at the end of each run. The clock was synchronized with the control PC. The photovoltaic array power input was monitored using two separate circuits for the voltage and current respectively. For the voltage, a 27 to 1 voltage divider circuit was wired in parallel to the photovoltaic circuit at the disconnect switch, and the resulting analog signal was sent to another Seeeduino microcontroller before being sent to the PC. A Deltec 100 mVDC:100 ADC shunt was installed on the negative leg of the photovoltaic circuit at the disconnect switch. The DC signal from the shunt was sent to a Texas Instruments INA282 low-side voltage output current shunt monitor to boost the signal to a readable level for the microcontroller to convert the signal to digital and send it to the PC for logging. Voltage at the PV disconnect contacts and current at the shunt were verified with a Fluke multimeter (Fluke 115 True RMS multimeter) and a further verification on the current reading was accomplished with a Fluke split-core current transformer (Fluke i410 AC/DC Current Clamp), with accuracies of 0.5% and 3.5% respectively. The Fluke multimeter was used to intermittently verify these same readings

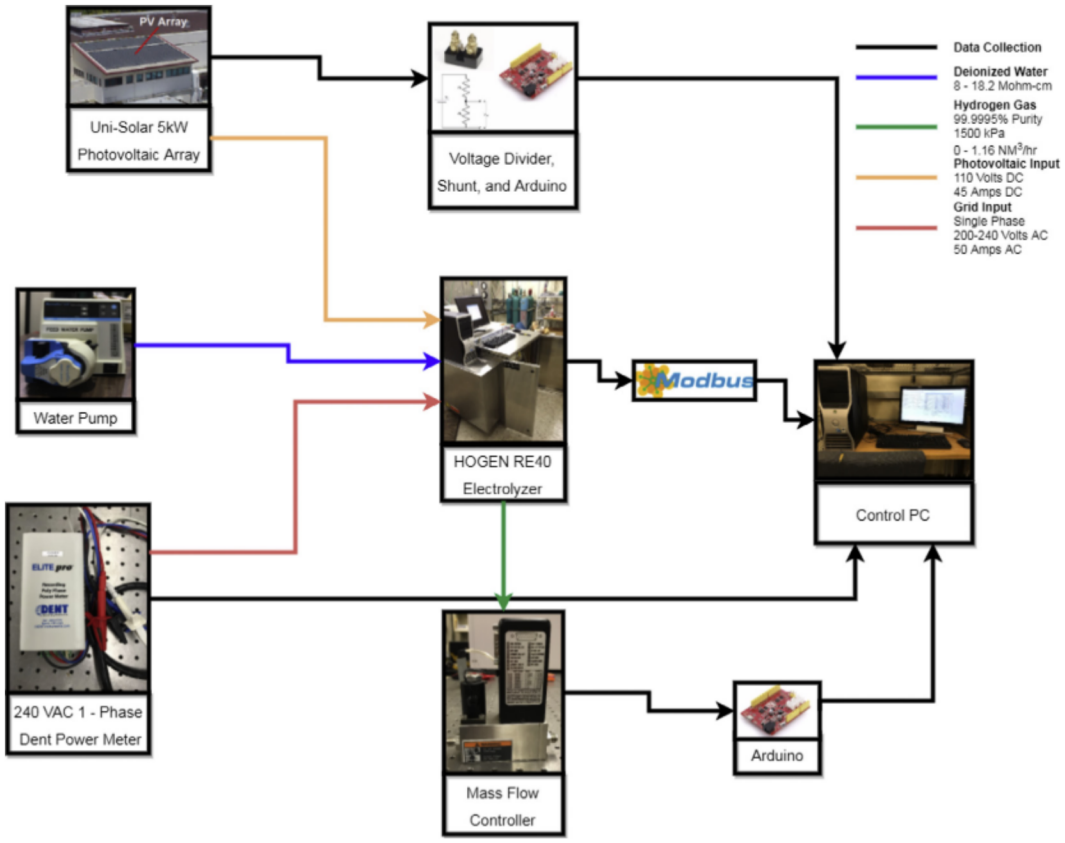

Fig. 3 – Proton OnSite HOGEN RE40 at the National Fuel Cell Research Center test facility – Experiment Layout.

during experiments to prevent any calibration errors over time.

Experimental methods

Pre-test conditioning

Upon receipt of the HOGEN RE40 system, pre-test conditioning was carried out to ensure that the system was operational and configured to manufacturer specifications. The system was deemed operational once it was able to run for a complete 12 h cycle in PV-only, and again in Grid-only mode. Hydrogen produced during pre-test conditioning was vented.

Steady state measurements

The system was run in short (~1–2 h) cycles in both Grid-only and PV-only mode to determine the average time to reach steady state operation from a 'cold start'. Steady state stack behavior during steady state operation was captured by establishing the stack voltage vs. current behavior across multiple steady-state tests. Efficiency of both the stack itself and the entire system was determined using 1st law analysis shown in Eqs. (1) and (2), where stack power refers to the power in watts consumed by the electrolysis cell stack, grid power refers to the electrical power measured from the grid input to the electrolyzer, the hydrogen mass flow is provided by the Brooks mass flow controller in kg/s, and the higher heating value of hydrogen is taken as 144 MJ/kg.

$$Eff_{Stack} = \frac{Energy\ \ Out}{Energy\ \ In} = \frac{\dot{m}_{H_2} * HHV_{H_2}}{Stack\ \ Power} \quad (1)$$

$$Eff_{System} = \frac{Energy\ \ Out}{Energy\ \ In} = \frac{\dot{m}_{H_2} * HHV_{H_2}}{Stack\ \ Power + Grid\ \ Power} \quad (2)$$

The system losses during both modes of operation were looked at and compared to generate a complete characterization of both modes of operation.

Testing in this phase was very similar to previous efforts at the U.S. Department of Energy's National Renewable Energy Laboratory (NREL) with the same HOGEN RE40 system. As such, results served to 'benchmark' system performance against their findings as well as to validate them. A few cycles incorporated tank filling, where the hydrogen process out was connected to a 35.68 L gas cylinder up to 1500 kPa. When a tank was not being filled, the hydrogen process stream was sent out the laboratory building ventilation system.

Transient performance

Transient state operation performance of the electrolyzer system is a critical characteristic of the electrolyzer system sought after for power-to-gas applications that are meant to complement renewable power dynamics (intermittency). Transient performance testing was carried out after

establishing an idea of the systems limits through the steady state testing phase. Tests were carried out under a variety of weather conditions in PV-only mode to get a variety of transient power input conditions from the photovoltaic system. Common failure states (i.e., those under which power provided to the stack was insufficient to continue producing hydrogen) and the underlying reasons behind these were characterized. Tests were carried out in the early morning until late evening on days with little to no-cloud coverage where intermittent failure did not occur. More dynamic and challenging solar conditions, such as marine layer conditions, were carried out until a consistent system failure point was identified.

Results and discussion

Stack performance

Electrolyzer stack performance is typically characterized by the j-V 'polarization' curve, which correlates the individual cell voltage in the stack with the current density, in mA/cm^2. Cell voltage and current density is assumed to be uniform across the entire stack. Cell voltage and current density values presented here are derived average values determined by stack voltage and current readings divided across the 20 cells in the stack with the knowledge of the active area of the stack.

Fig. 4 presents a j-V curve generated from three separate steady-state operating conditions of the electrolyzer system. Grid-only mode operation can be seen at the upper range of the curve, at the electrolyzer's maximum current density of 1.50 A/cm^2 and operating in a voltage range of 2.08–2.15 V per cell. Two experiments of the PV-only mode, one conducted in August of 2015 and another in November, show a clear disparity in stack performance. In August, the stack performed more efficiently, operating at a lower cell voltage per unit of additional current density as compared to the November conditions.

Aggregating stack voltage and current readings across the entirety of the acquired data and then correlating all the data points to the operating temperature (measured at the water outlet of the stack) show the correlation between stack efficiency and operating temperature in Fig. 5. This observed performance trend is most likely due to increased ionic conductivity in the electrolytic membrane and/or reduced activation polarization as a result of the higher temperature [19,51].

Normal electrolyzer operation introduces heat into the system, and as such, an in-situ performance increase can be observed as the system 'warms up'. Calculating and plotting stack efficiency as per Eq. (1), we can observe (Fig. 6) an increasing efficiency trend upon start-up at steady current density that roughly tracks the increasing system temperature. Throughout experimental analyses, stack efficiency typically varied between 52 and 62% during operation, primarily as a function of current density with slight increases as a function of system temperature only, regardless of whether photovoltaic power or grid power was utilized.

System losses characterization – 'grid only' vs. 'PV only' operation

Of interest to the coupling of renewable energy sources to electrolysis are the possible advantages of direct DC electricity usage to mitigate efficiency losses from power conversion and conditioning. Photovoltaic solar panels and some wind turbines produce DC electricity, which is typically fed to an inverter that converts DC electricity to AC for grid integration. Electrolysis is a DC electricity process, and in the event that the electrolysis system is situated near the photovoltaics, elimination of AC/DC conversion is attractive. The performance of the HOGEN40 power conditioning steps and

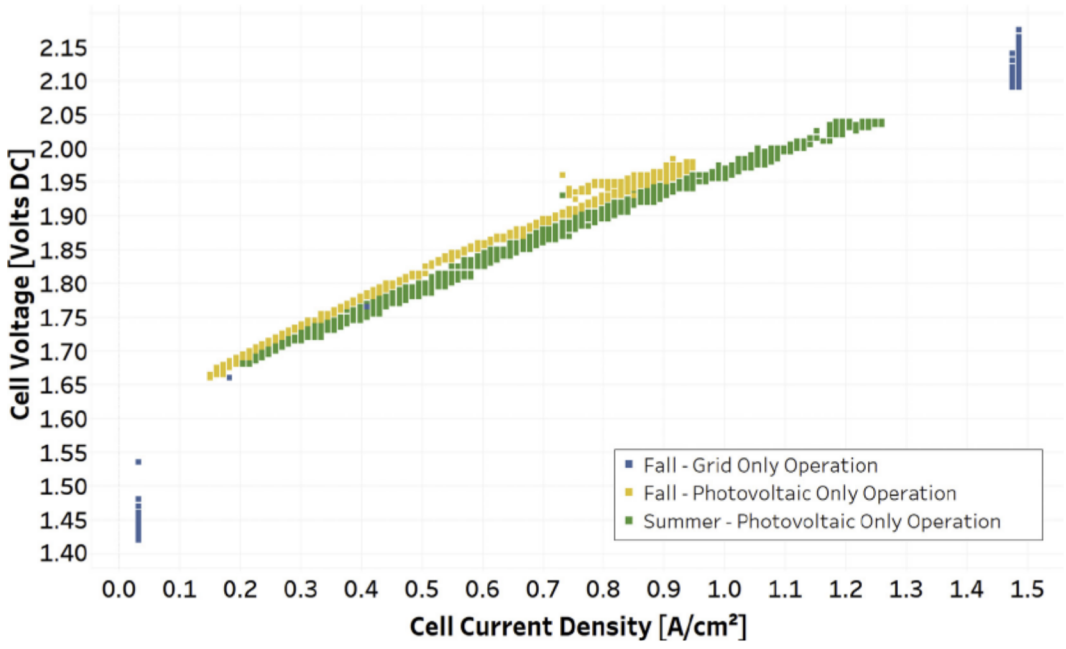

Fig. 4 – HOGEN RE40 cell stack polarization curve, seasonal performance comparison.

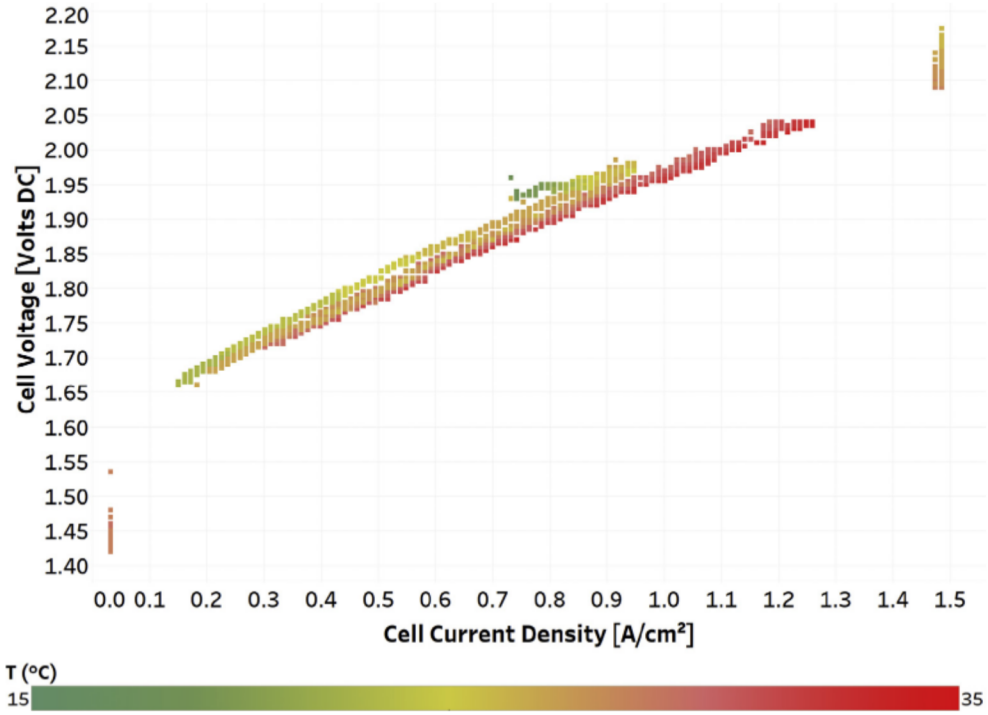

Fig. 5 – HOGEN RE40 polarization curve for various stack temperature operating conditions.

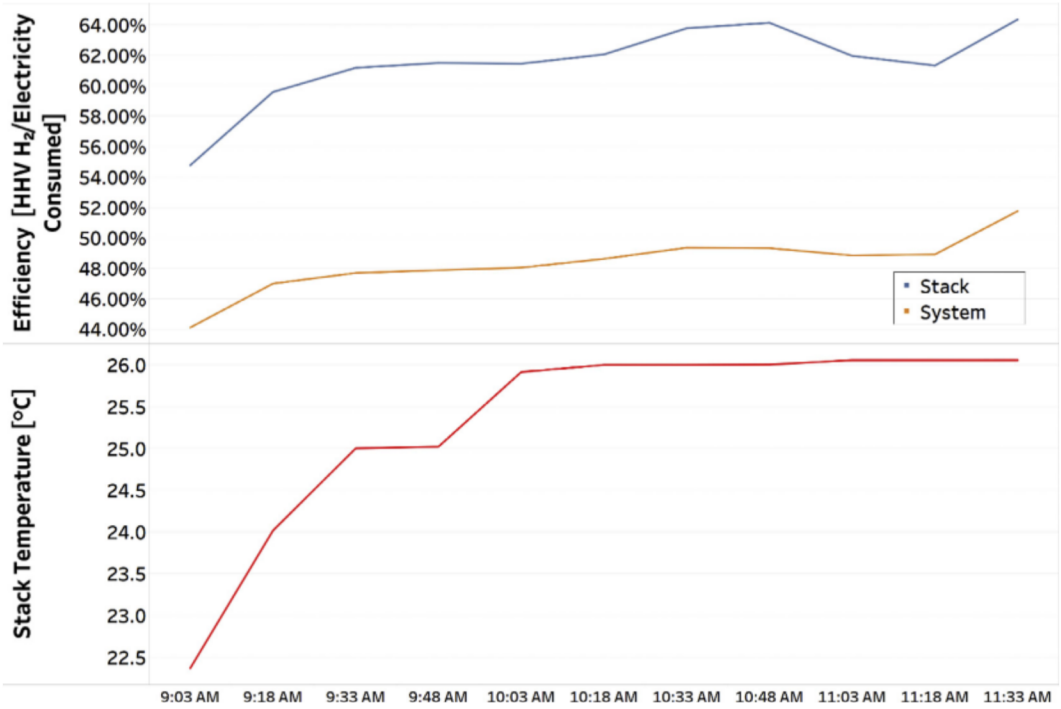

Fig. 6 – In-situ 'warm-up' effect of the stack. Stack temperature vs. system and stack efficiency.

hydrogen drying process in AC grid-only mode vs. DC input in PV-mode are shown in Figs. 7 and 8 respectively. Fig. 7 displays the power consumption trends of 'Grid-Only' operation from the entire system, the power sent to the stack before AC/DC power conditioning, stack power after AC/DC power conditioning, and the resultant hydrogen flow before and after the drying process. Fig. 8 shows the power consumption for 'PV-Only' mode for the entire system, the photovoltaic power input before DC/DC power conditioning, stack power after DC/DC power conditioning, and the resultant hydrogen flow

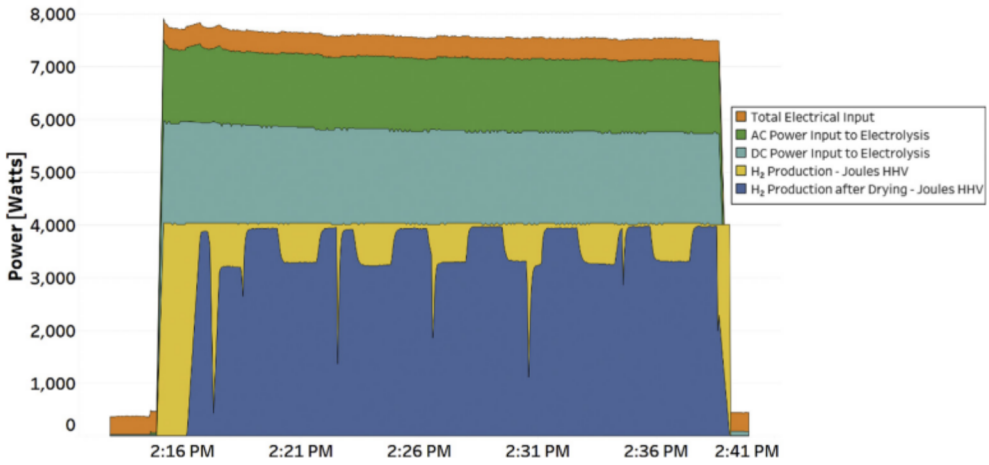

Fig. 7 – Grid-only power source to electrolysis power conditioning behavior.

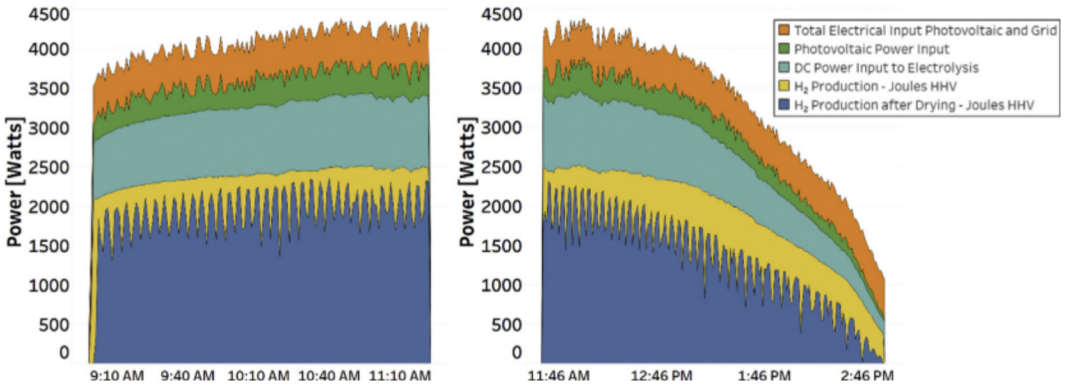

Fig. 8 – PV-only power source to electrolysis power conditioning behavior. Ramp up and ramp down.

before and after the drying process for both a 'ramp up' solar scenario and a 'ramp down' solar scenario. Hydrogen flow is represented as the higher heating value in joules of hydrogen produced per second, or in 'watts' higher heating value of hydrogen gas produced, to illustrate the magnitude of the energy conversion steps from electricity to hydrogen.

In Grid-only operation, the 240 VAC single phase input goes through an AC/DC rectifier, which converts the AC electricity to the DC electricity that the stack can utilize. Fig. 7 shows the typical duration of operation (approximately 25 min) needed for the system to reach an operating temperature of 36 °C from a starting point of 21 °C. 36 °C is the temperature the system typically would equilibrate at in the NFCRC test environment and this condition exhibited the highest efficiency at maximum current density. The stack is able to operate at the rated input of 6000 W when pulling from the grid (2:16pm) and slightly drops to 5700 W (2:41pm) as the stack warms up and is able to operate more efficiently after warming up completely. Overall power input to the system starts at 7800 W and drops to around 7500 W as the electrolysis process becomes more efficient. Ancillary system loads demand around 400 W. The AC/DC rectification circuit operates consistently on 100 W at an efficiency of 81%, for a net loss of 1400 W of electrical power when the electrolyzer is at full load condition. The 'swing bed' PSA dryers result in an additional parasitic loss of hydrogen production, as some is vented out during dryer operation. Efficiency measures are assessed with the 'dried' hydrogen and thus account for dryer losses.

On average, stack efficiency during Grid-only operation was 53.72%. System efficiency was 40.68% for a consumption rate of 98.3 kWh/kg H_2. In PV-only operation, average stack efficiency was 56.57% and system efficiency averaged 47.68%. Discrepancy in stack performance can be attributed to part load operation in PV-only, at maximum output from the photovoltaic array the HOGEN RE40 could only go as high as 70% part load capacity, whereas Grid-only consistently operated at 90% and higher. As a result of lower part load operation, lower current densities result in higher performance in stack efficiency due to reduction of electrode and ohmic overpotential losses [52,53]. Reduced losses in power conditioning to the electrolysis process in combination with lower current densities together contributed to better system efficiencies in PV-only operation. Grid-only runs did benefit performance-wise from typically higher system temperatures produced from operating at higher current density. The effect was more pronounced compared to photovoltaic operation in

fall and winter months where a combination of lower ambient temperatures and less overall energy throughput could make a sustained system temperature operating difference of as much as 10 °C between the two operational modes.

In 'PV-Only' operation, a DC-DC buck converter takes in DC electricity within a rated voltage range of 60–200 VDC and outputs DC electricity at the stack voltage set point of 40 VDC. Ancillary system power demands are identical to Grid-only, the difference in power consumption of the DC-DC buck converter compared to the AC/DC rectifier is negligible. For the PV-only mode assessment shown in Fig. 8, the system was run for roughly 6 h. Over the course of operation, the system consumed 18.0 kWh, of which 15.3 kWh went to the cell stack for electrolysis. A total of 0.225 kg of hydrogen containing 9.02 kWh of energy was produced, for an average system efficiency of 49.3% and a stack efficiency of 58.3%. The resultant system consumption rate under these conditions was 80.1 kWh/kg H_2. As solar waned towards the end of the day, the system was able to maintain a part load condition as low as 7.6%. PV-only power conversion losses are characterized by the performance of the DC-DC power electronics. Fig. 9 shows that the efficiency of the DC-DC process varied between 86 and 94%. Our tests indicate that higher input voltages from the photovoltaic array were correlated with lower efficiencies. NREL tested the system DC-DC buck converter via a controllable DC power source before receipt of the system by the National Fuel Cell Research Center and obtained similar results [54].

System dynamic performance under transient conditions

Successful coupling of renewable energy sources to a PEM electrolyzer demands rapid ramping capabilities of the electrolyzer system in the event of highly intermittent scenarios. Fig. 10 presents data from PV-only operation for marine layer conditions, common in southern California, which are representative of one 'extreme' of solar power intermittency for assessing the HOGEN RE40 connected directly to solar photovoltaic load. The power dynamics of the stack, coming from the photovoltaic system through the DC/DC conditioning step, and the power demand of the ancillary services coming from the grid, were tracked against resultant hydrogen flow. Hydrogen flow is calculated on a higher heating value basis from the mass flow measurements to clearly demonstrate the energy dynamics of the system. The roughly 7-min period 'swinging' of the hydrogen production is due to the hydrogen drying process, which results in intermittent flow when switching between dryer beds.

On October 14th, 2015, the electrolyzer system was operated in PV-only mode during intermittent cloud coverage. Weather conditions resulted in highly transient photovoltaic array behavior. For a run time of 4 h and 12 min, the system operated continuously with power input varying from 4500 W DC to as low as 1000 W DC to the electrolysis process, a part load condition ranging from 15% to 70%. Ramp rates as high as 1270 W/s were observed as the electrolyzer responded to transient cloud coverage. The system consumed 13.0 kWh, with 10.9 kWh going to the stack, to produce a total of 0.15 kg H_2 or 6.00 kWh HHV basis. System efficiency averaged 46.1% and stack efficiency averaged 54.9%. Transient power input conditions were well handled by the PEM electrolyzer and only appeared to have a slight (2–3%) impact on stack efficiency as compared to a typical 'smooth' photovoltaic profile.

Threshold operation and failure states with direct PV input

The system start-up behavior and operational behavior at threshold power input conditions were examined to assess the factors that could affect start-up times and performance under highly dynamic conditions (e.g., multiple start-up,

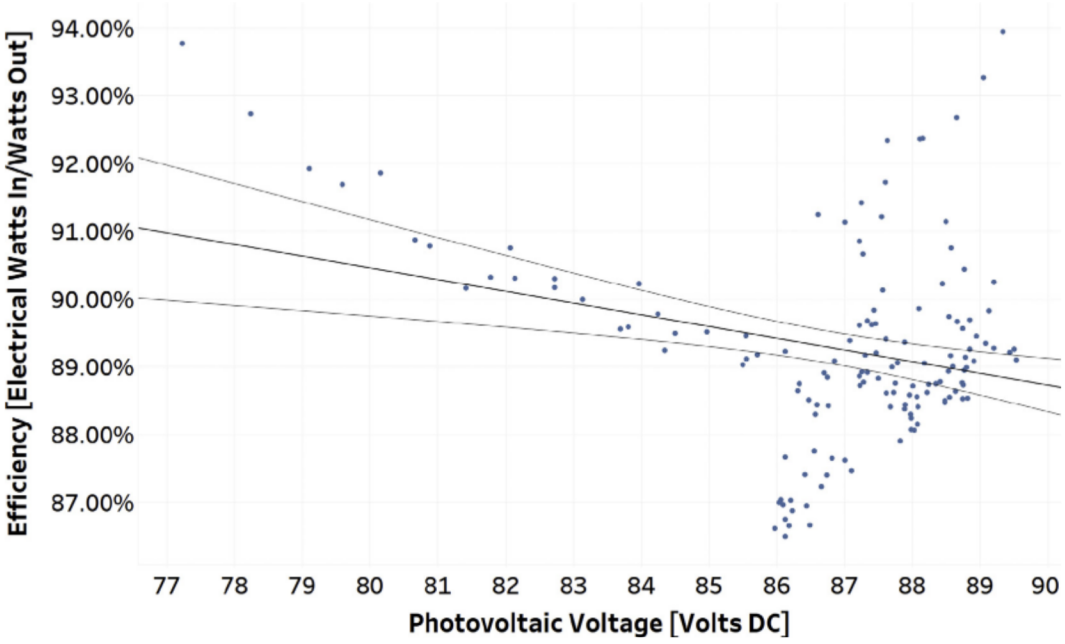

Fig. 9 – DC/DC Buck Converter w/MPPT Optimization Efficiency vs. Photovoltaic Voltage.

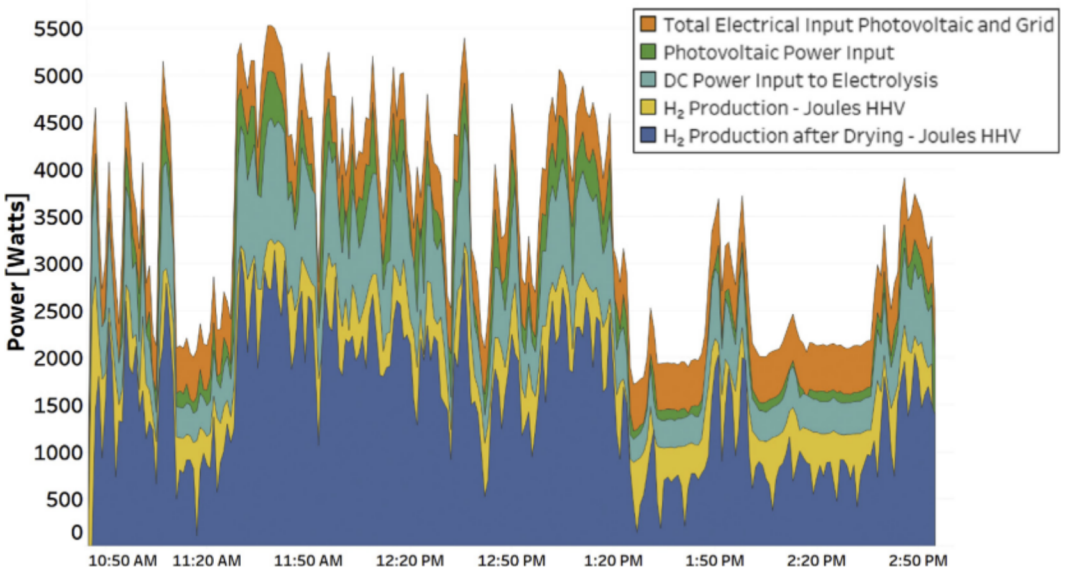

Fig. 10 – Power consumption of the stack and ancillary services of the HOGEN RE40 for high transience solar conditions.

shut-down conditions to complement intermittent renewable power). Factors affecting the occurrence of system failure were similarly investigated during these tests. Both characteristics are of interest to electrolyzer coupling with solar energy, where concerns of repeated start up and system failure arise when considering the sometimes extreme intermittency of solar energy in the event of cloud cover. The primary pathway by which failure was assessed was via stack power input, as this remains the most dynamic variable due to its dependence upon solar energy availability.

Start-up failure of the HOGEN electrolyzer system largely depends upon set point conditions. The most common failure state associated with start-up, with default set point conditions, was identified as a low stack pressure error. When entering into electrolysis, the stack was required to first reach the set point pressure before it can begin flowing hydrogen out to the process port. The HOGEN is configured to enter a failure state if the 'low' product pressure set point is not reached within 30 s of start-up and is subsequently maintained. Tests were carried out with the 'low' pressure set point at 200psig so as to analyze the threshold stack conditions where start-up of the system could fail due to low solar energy conditions. Fig. 11 displays the j-V curve of the stack during threshold operation testing. Failure states were gathered on November 2, 2015 as heavy cloud cover rolled through the area starting at noon. Start-up failure occurred at stack power inputs as high as 2000 W down to 900 W, for minimum start up part load condition of 33.9%. Successful start-up occurred at points as low as 3800 W, a part load condition 58.5%. On November 19th during transient solar condition testing, start-up was achieved at 2330 W, the lowest observed stack power input to achieve start up. For reliable system start-up and subsequent product delivery at a given pressure to occur, a minimum part load condition of 35.8% was observed across all of the experiments conducted.

The part load condition operation range of the HOGEN when operating at a 1380 kPa product minimum pressure has been observed to go as low as 7.6%, which is lower than observed minimum part load condition required for system start-up. Fig. 12 illustrates the occurrence when successful system operation is interrupted, and then start-up is reattempted. Successful start-up occurred with intermittent solar conditions that had an average electricity throughput of 3000 W. Incident cloud coverage shortly after start up resulted in a dramatic drop in PV output to the stack. The system was stopped and allowed to depressurize. Attempts to start the system up again were unsuccessful, as the stack was unable to pressurize within the 30-s time period. The highest part load condition at which start-up failure was observed occurred at an average 23.1% part load condition (1459.6 W).

Discussion

A 7000 W PEM electrolysis system with DC-DC power conditioning capabilities has been operated and tested with both photovoltaic and grid power electrolysis to assess the viability of such a system for future power-to-gas efforts that complement intermittent renewable power. Stack and system efficiency as well as dynamics were studied, as well as the characteristic losses associated with both DC electrical input and AC electrical input to the electrolysis process. Threshold studies to determine the operability of the photovoltaic coupled system under transient conditions were undertaken as well.

Electrolyzer stack performance was most affected by operating temperature, with a noticeable improvement of performance due to waste heat from the electrochemical process driving up the system's temperature as it continued to operate. Dynamics of the DC power input to the electrolysis process did not have any pronounced effect on stack performance, and the system was able to rapidly follow highly transient solar conditions without failure. System performance gains were observed by as much as 7–8% efficiency when utilizing DC electrical input, primarily due to efficiency

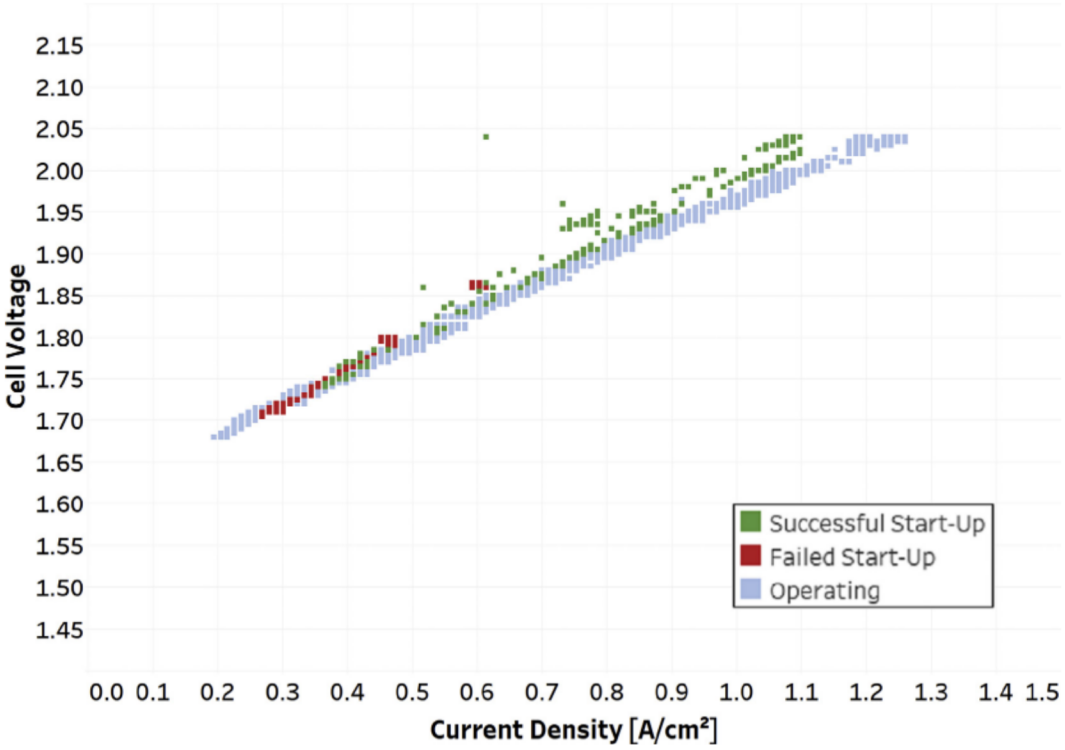

Fig. 11 – Analysis of stack I-V profile for successful start-up power input regimes.

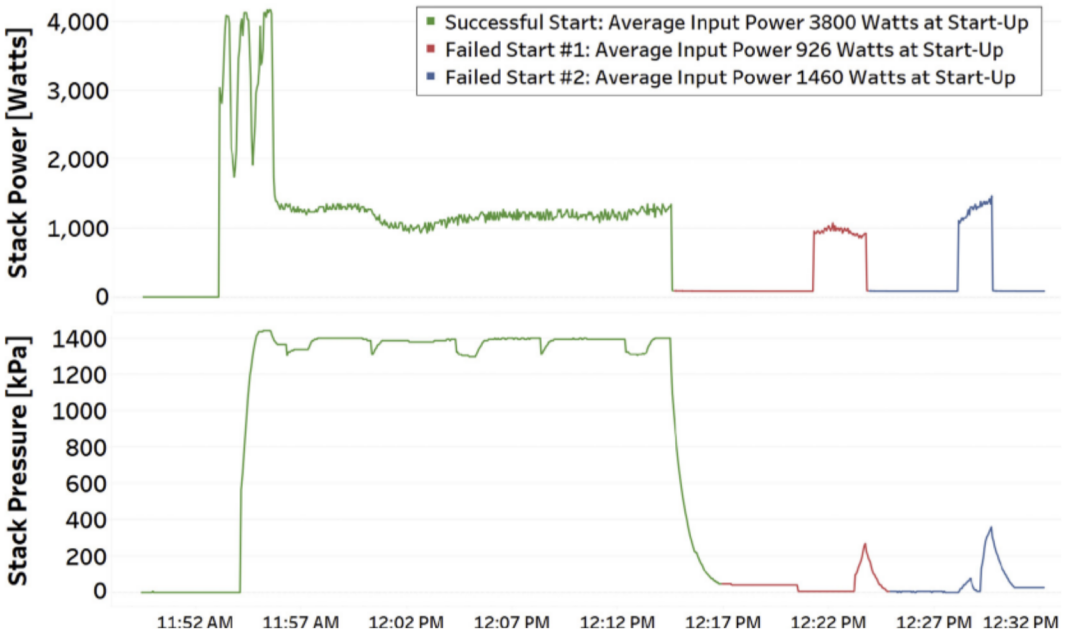

Fig. 12 – Threshold start-up analysis on low pressure start up failures.

losses associated with the AC/DC rectification process when using AC electricity for electrolysis. Larger, state of the art systems typically utilize 3-phase AC electricity input that have higher efficiency AC/DC conditioning power electronics. The DC/DC conversion process is more efficient overall. Future work on such systems would shine a better light on the relative benefits of DC/DC power electronics versus AC/DC conversion.

Transient operation of the system demonstrated that as low as 7.6% part load power could support continued operation. System start up failed at part load conditions as high as 33.85%. This indicates that when considering these systems

for integration with power-to-gas, threshold losses from delayed start up need to also be considered, as the full range of part load condition operation is only available once the system has been pressurized. A cold-start of the system typically took 8–12 min in PV-only, dependent on the power throughput to the stack as it pressurized upon start-up. Warm-starts, such as that investigated on November 19, behaved much the same.

For PEM fuel cells, the integration of a battery energy system has great complementary characteristics for handling the more extreme transience operating conditions [55]. Likewise, hybrid energy storage systems, with the integration of battery, supercapacitor or grid import/export, could seemingly eliminate these start-up threshold losses by capturing energy below the minimum start up conditions or providing a jump start of sorts to the system, ultimately resulting in improved energy management [56,57]. Today, PEM electrolysis systems are becoming increasingly efficient, with stack efficiencies typically in the range of 65–85% as well as the ability to operate at increasingly higher differential pressures [21,22,58]. This increase in efficiency and output pressure with the dynamics of the system itself make PEM electrolysis an increasingly competitive option for the power-to-gas concept and implementation of a hydrogen infrastructure. The utilization of DC-DC electricity conditioning technology in solar PV integrated electrolysis with MPPT power electronics as demonstrated in this study could have benefits over traditional solar PV to electrolysis approaches. This supports similar findings carried about by NREL [59].

Hydrogen technology implementation is becoming increasingly feasible and will lead to a reduction in greenhouse gas and criteria pollutant emissions, as well as reducing foreign dependence on fossil fuels when generated from renewable electrolysis. Power-to-gas provides a pathway for hydrogen to steadily integrate with existing energy infrastructure in a renewable manner and provide the benefits of grid scale energy storage that increasing amounts of renewable energy generation ultimately will demand.

Summary and conclusions

Under steady-state operating conditions the stack temperature was found to have a significant impact on the PEM electrolyzer polarization curve. Operating the stack in highly transient solar conditions did little to affect efficiency, and the system was able to rapidly follow highly transient solar conditions without failure. System performance gains were observed by as much as 7–8% efficiency when utilizing DC electrical input. Transient operation of the system demonstrated that as low as 7.6% part load condition could support continued operation, but, system start up failed at part load conditions as high as 33.9% part load.

Funding

This work was supported by the National Fuel Cell Research Center at the University of California Irvine; and the Southern California Gas Company.

Acknowledgements

The authors thank Eric Pedersen, posthumously, for laying the foundation for this work. Your endless enthusiasm for discovery and progress serves as an inspiration every day. Our deepest gratitude also goes to the memory of Richard Hack for assistance on the installation of the electrolyzer system and the design of the data acquisition systems used.

REFERENCES

[1] Beiter P, Haas K, Buchanan S. 2014 renewable energy data book. United States Department of Energy; 2015.
[2] Bird L, Lew D, Milligan M, Carlini ME, Estanqueiro A, Flynn D, et al. Wind and solar energy curtailment: a review of international experience. Renew Sustain Energy Rev 2016;65:577–86.
[3] Bird L, Cochran J, Wang X. Wind and solar energy curtailment: experience and practices in the United States. National Renewable Energy Laboratory; 2014.
[4] Megerian C. Los Angeles Times. 23 March 2015 [Online]. Available: http://www.latimes.com/local/politics/la-me-pol-green-energy-20150324-story.html. [Accessed 24 January 2016].
[5] California Public Utilities Commission. "California renewables portfolio standard (RPS)," State of California. 2016 [Online]. Available: http://www.cpuc.ca.gov/RPS_Homepage/. [Accessed 24 January 2016].
[6] California Energy Commission. Staff draft report on renewable power in California: status and issues. 2011. Publication No. CEC-150-2011-02.
[7] Energy and Environmental Economics. "Investigating a higher renewables portfolio stand in California," San Francisco, CA. 2014.
[8] Budischak C, Sewell D, Thomson H, Mach L, Veron DE, Kempton W. Cost-minimized combinations of wind power, solar power and electrochemical storage, powering the grid up to 99.9% of the time. J Power Sources 2013;(225):60–74.
[9] Elliston B, Diesendorf M, MacGill I. Simulations of scenarios with 100% renewable electricity in the Australian national electricity market. Energy Policy 2012;45:606–13.
[10] Tarroja B, Mueller F, Eichman JD, Samuelsen S. Metrics for evaluating the impacts of intermittent renewable generation on utility load-balancing. Energy 2012;42:546–62.
[11] Beaudin M, Zareipour H, Schellenberg A, Rosehart W. Energy storage for smart grids (Ch1. Energy storage for mitigating the variability of renewable electricity resources), department of electrical and computer engineering, university of calgary, 2500 university drive NW, Calgary, Alberta, Canada T2N 1N4. Elsevier Inc.; 2015.
[12] Schaaf T, Grunig J, Schuster MR, Rothenfluh T, Orth A. Methanation of CO_2-storage of renewable energy in a gas distribution system. Energy Sustain Soc 2014;4.
[13] Walker SB, Mukherjee U, Fowler M, Elkamel A. Benchmarking and selection of power-to-gas utilizing electrolytic hydrogen as an energy storage alternative. Int J Hydrogen Energy 2016;41(19):7717–31.
[14] Gahleitner G. Hydrogen from renewable electricity: an international review of power-to-gas pilot plants for stationary applications. Int J Hydrogen Energy 2013;38(5):2039–61.
[15] Maton J-P, Zhao L, Brouwer J. Dynamic modeling of compressed gas energy storage to complement renewable

wind power intermittency. Int J Hydrogen Energy 2013;38(19):7867–80.
[16] Estermann T, Newborough M, Sterner M. Power-to-gas systems for absorbing excess solar power in electricity distribution networks. Int J Hydrogen Energy 2016;41(32):13950–9.
[17] Akhil AA, Huff G, Currier AB, Kaun BC, Rastler DM, Chen SB, et al. DOE/EPRI electricity storage handbook in collaboration with NRECA. Sandia National Laboratories; 2015.
[18] Russell JH, Nuttall LJ, Fickett AP. Hydrogen Generation by solid polymer electrolyte water electrolysis. Am Chem Soc Div Fuel Chem Prepr 1973;18(3):24–40.
[19] EG&G Technical Services. Fuel cell handbook. 26507–0880. 7th ed. Morgantown, West Virginia: U.S. Department of Energy, Office of Fossil Energy, National Energy Technology Laboratory; 2004.
[20] Millet P, Mbemba N, Grigoriev S, Fateev V, Aukauloo A, Etievant C. Electrochemical performances of PEM water electrolysis cells and perspectives. Int J Hydrogen Energy 2011;36(6):4134–42.
[21] Siracusano S, Baglio V, Briguglio N, Brunaccini G, Di Blasi A, Stassi A, et al. An electrochemical study of a PEM stack for water electrolysis. Int J Hydrogen Energy 2012;37(2):1939–46.
[22] Felgenhauer M, Hamacher T. State-of-the-art of commercial electrolyzers and on-site hydrogen generation for logistic vehicles in South Carolina. Int J Hydrogen Energy 2015;40(5):2084–90.
[23] Carmo M, Frtiz DL, Mergel J, Stolten D. A comprehensive review on PEM water electrolysis. Int J Hydrogen Energy 2013;38(12):4901–34.
[24] Han B, Steen III SM, Mo J, Zhang F-Y. Electrochemical performance modeling of a proton exchange membrane electrolyzer cell for hydrogen energy. Int J Hydrogen Energy 2015;40(22):7006–16.
[25] Aouali FZ, Becherif M, Ramadan HS, Emziane M, Khellaf A, Mohammedi K. Analytical modelling and experimental validation of proton exchange membrane electrolyser for hydrogen production. Int J Hydrogen Energy 2017;42(2):1366–74.
[26] Grigoriev SA, Kalinnikov AA. Mathematical modeling and experimental study of the performance of PEM water electrolysis cell with different loadings of platinum metals in electrocatalytic layers. Int J Hydrogen Energy 2017;42(3):1590–7.
[27] Abdin Z, Webb CJ, Gray EM. Modelling and simulation of a proton exchange membrane (PEM) electrolyser cell. Int J Hydrogen Energy 2015;40(39):13243–57.
[28] Li X, Qu S, Yu H, Hou M, Shao Z, Yi B. Membrane water-flow rate in electrolyzer cells with a solid polymer electrolyte (SPE). J Power Sources 2009;190:534–7.
[29] Lee B, Park K, Kim H-M. Dynamic simulation of PEM water electrolysis and comparison with experiments. Int J Electrochem Sci 2013;8:235–48.
[30] Schalenbach M, Carmo M, Fritz DL, Mergel J, Stolten D. Pressurized PEM water electrolysis: efficiency and gas crossover. Int J Hydrogen Energy 2013;38(35):14921–33.
[31] Görgün H. Dynamic modelling of a proton exchange membrane (PEM) electrolyzer. Int J Hydrogen Energy 2006;31(1):29–38.
[32] Kim H, Park M, Lee KS. One-dimensional dynamic modeling of a high pressure water electrolysis system for hydrogen production. Int J Hydrogen Energy 2013;38(6):2596–609.
[33] Olivier P, Bourasseau C, Bouamama B. Dynamic and multiphysics PEM electrolysis system modelling: a bond graph approach. Int J Hydrogen Energy 2017;42(22):14872–904.
[34] Laoun B, Khellaf A, Naceur MW, Kannan AM. Modeling of solar photovoltaic-polymer electrolyte membrane electrolyzer direct coupling for hydrogen generation. Int J Hydrogen Energy 2016;41(24):10120–35.
[35] Sarrias-Mena R, Fernández-Ramírez LM, García-Vázquez CA, Jurado F. Electrolyzer models for hydrogen production from wind energy systems. Int J Hydrogen Energy 2015;40(7):2927–38.
[36] Saadi A, Becherif M, Ramadan HS. Hydrogen production horizon using solar energy in Biskra, Algeria. Int J Hydrogen Energy 2016;41(47):21899–912.
[37] Blal M, Ali B, Ahmed B, Ahmed B, Salah L, Rachid D. Study of hydrogen production by solar energy as tool of storing and utilization renewable energy for desert areas. Int J Hydrogen Energy 2016;41(45):20788–806.
[38] Zhao L, Brouwer J. Dynamic operation and feasibility study of a self-sustainable hydrogen fueling station using renewable energy sources. Int J Hydrogen Energy 16 March 2015;40(10):3822–37.
[39] Maclay JD, Brouwer J, Samuelsen GS. Dynamic analyses of regenerative fuel cell power for potential use in renewable residential applications. Int J Hydrogen Energy July 2006;31(8):994–1009.
[40] Özgirgin E, Devrim Y, Albostan A. Modeling and simulation of a hybrid photovoltaic (PV) module-electrolyzer-PEM fuel cell system for micro-cogeneration applications. Int J Hydrogen Energy 2015;40(44):15336–42.
[41] Genç G, Çelik M, Genç MS. Cost analysis of wind-electrolyzer-fuel cell system for energy demand in Pinarbaşi-Kayseri. Int J Hydrogen Energy 2012;37(17):12158–66.
[42] Kotowicz J, Bartela Ł, Węcel D, Dubiel K. Hydrogen generator characteristics for storage of renewably-generated energy. Energy 2017;118:156–71.
[43] Ramsden T, Harrison K, Steward D. NREL wind to hydrogen project: renewable hydrogen production for energy storage & transportation. 2009. NREL/PR-560-47432, Golden, CO.
[44] Eichman J, Harrison K, Peters M. Novel electrolyzer applications: providing more than just hydrogen. 2014. NREL/TP-5400–61758, Golden, CO.
[45] Santarelli M, Medina P, Cali M. Fitting regression model and experimental validation for a high-pressure PEM electrolyzer. Int J Hydrogen Energy 2009;34(6):2519–30.
[46] Schiebahn S, Grube T, Robinus M, Tietze V, Kumar B, Stolten D. Power to gas: technological overview, systems analysis and economic assessment for a case study in Germany. Int J Hydrogen Energy 2015;40(12). 4285–2494.
[47] Mergel J, Carmo M, Fritz D. In: Stolten D, Scherer V, editors. Status on technologies for hydrogen production by water electrolysis. Weinheim, Germany: WILEY-VCH; 2013.
[48] Gibson TL, Kelly NA. Optimization of solar powered hydrogen production using photovoltaic electrolysis devices. Int J Hydrogen Energy 2008;33(21):5931–40.
[49] Harrison K, Martin G, Ramsden T, Kramer B. The wind-to-hydrogen project: operational experience, performance testing, and systems integration. National Renewable Energy Laboratory; 2009. NREL/TP-581–44082.
[50] Maclay JD, Brouwer J, Samuelsen GS. Experimental results for hybrid energy storage systems coupled to photovoltaic generation in residential applications. Int J Hydrogen Energy 2011;36(19):12130–40.
[51] Ni M, Leung MK, Leung DY. Electrochemistry modeling of proton exchange membrane (PEM) water electrolysis for hydrogen production. In: World hydrogen energy conference, Lyon, France; 2006.
[52] Paidar M, Fateev V, Bouzek K. Membrane electrolysis - history, current status and perspective. Electrochem Acta 2016;209:737–56.
[53] Suermann M, Schmidt TJ, Büchi FN. Cell performance determining parameters in high pressure water electrolysis. Electrochimica Acta 2016;211:989–97.

[54] Harrison K. S40 RE electrolyzer testing (TSA-15–699). 2015.
[55] Zhao L, Brouwer J, James S, Siegler J, Peterson E, Kansal A, et al. Dynamic performance of an in-rack proton exchange membrane fuel cell battery system to power servers. Int J Hydrogen Energy 13 April 2017;42(15):10158–74.
[56] Hemmati R, Saboori H. Emergence of hybrid energy storage systems in renewable energy and transport applications - a review. Renew Sustain Energy Rev 2016;65:11–23.
[57] Tamalouzt S, Benyahia N, Rekioua T, Rekioua D, Abdessermed R. Performance analysis of WT-DFIG with PV and fuel cell hybrid power sources system associated with hydrogen storage hybrid energy system. Int J Hydrogen Energy 2016;41(45):21006–21.
[58] Hamdan M. High pressure PEM electrolysis: status, key issues, and challenges. National Renewable Energy Laboratory; 2014.
[59] Steward D, Ramsden T, Harrison K. Hydrogen for energy storage analysis. Golden, Colorado: National Renewable Energy Laboratory; 2010.